

Orbital–Specific Exchange Potentials for Noble Gases and Nitrogen atom with Depurated Inversion of Hartree–Fock wavefunctions

M.P.A. Mendez, D.M. Mitnik, J.E. Miraglia *

October 20, 2019

Abstract

Exchange potentials for specific orbitals of noble gases are calculated by inverting the corresponding Hartree–Fock wavefunctions. This approach was performed by using a *Depurated Inversion Method*, which is presented here. The basic idea of the method relies upon the substitution of Hartree–Fock orbitals and eigenvalues into the Kohn–Sham equation. Through inversion, the corresponding effective potential were obtained. A further depuration of the potential should be performed. It consists in a careful optimization which eliminates the poles and also ensures the fulfillment of the appropriate boundary conditions. The procedure developed here is not restricted to the ground state or to a nodeless orbital and is applicable to any kind of atom. As an example, exchange potentials for the term–dependent orbitals of the lower configuration of Nitrogen are also calculated. The method allows to reproduce the input energies and wavefunctions with a remarkable degree of accuracy.

*Instituto de Astronomía y Física del Espacio, CONICET–UBA, Buenos Aires, Argentina.

1 INTRODUCTION

The successful idea of replacing the many-body, non-local interaction by an effective one-electron equation opened up the possibility of studying extremely complex systems with high accuracy. In this context, the success of the Kohn–Sham density–functional theory began when crucial developments in its exchange–correlation term gave the theory predictive power competitive with well-developed wavefunction methods¹. The importance of the exchange–correlation potentials in chemical physics has been emphasized by Bartlett^{2,3}. Local potentials are mostly constructed by using the optimized effective potential (OEP) method^{4–11} or through the direct inversion of the Kohn–Sham equations (see, for example Kananenka *et al.*¹²). In general, these potentials are obtained with a weighted average of the different orbitals.

The atomic collision community, on the other hand, is also eager to accurately determine effective one-electron local potentials, allowing to generate in a simple way the wavefunctions of the particles interacting in a scattering process. In particular, they need to represent an orthonormal set of bound and continuum states to calculate the transition probabilities. Their necessities include detailed nl -orbital potentials, a characteristic missing in most of the standard density functional methods. Soft pseudopotentials like ABINIT¹³ or USPP¹⁴ cannot be used since they overlook the information of the internal region of the wavefunctions. The features of this region can play a very important role, such as the cusp conditions in the processes of electron capture and ionization. In an attempt to meet the needs of both chemist and collisionist communities, we strove to obtain accurate and simple specific nl -orbital local potentials.

How to determine central potentials from known electron wavefunctions and densities is a well studied subject in the DFT community^{15–17}. The extraction of the true Kohn–Sham exchange–correlation potential from near-exact electronic densities has been demonstrated, with particular reference to the two-electron systems like He¹⁸, He-isoelectronic ions¹⁹, and H₂^{18,20} as well as exact soluble models (for example, an external harmonic potential as in Filippi *et al.*²¹).

Some other works start with a particular Kohn–Sham potential and solve the corresponding equations, obtaining the KS orbitals^{15,22,23}. By inversion, they obtain a reconstructed KS potential, which coincides almost everywhere with the original one, excepting some regions where huge oscillations arise¹². In some cases, the reconstructed potential may be distorted beyond recognition^{18,24}. The same type of procedure was suggested many years ago by Hilton *et al.*^{25,26}, in applications circumscribed to the calculation of photoionization processes of atoms^{25,26}, water²⁷ and other molecules^{28,29}. These papers, in turn, refer to the earlier work in atomic polarizability by Sternheimer³⁰ and by Dalgarno and Parkinson³¹. However, they focused on the final photoionization cross section results, and they did not provide details about the quality of the potentials and the wavefunctions they generated.

Assuming the validity of the separation between exchange and correlation functionals, we will focus here only on the calculation of the exchange contribution to the potential. Since Hartree–Fock does not include the correlations, then, our approach allows to obtain the “exact” one-electron local potential representing the exchange interactions. Our strategy does not rely on the KS inversion formula, instead, we directly invert the Hartree–Fock solutions. That is, we solve a KS-type equation, but rather than having KS-orbitals, we

operate directly with the Hartree–Fock wavefunctions. For open–shell atoms, we will be able to find orbital spin–polarized exchange potentials, this being crucial, for instance, to find the hyperfine coupling constants^{32,33}.

However, this is not a simple task, and probably that is why the method presented here was not widely applied in the past. If the wavefunction has nodes, they will produce huge poles in the potential. Moreover, even for nodeless states, the asymptotic decaying behavior of the bound wavefunctions produces severe numerical difficulties, making the inversion operation intractable sometimes. In our method, a depuration procedure follows the inversion. This depuration implies, first, the annihilation of the poles. Then, a careful optimization of the potential which ensures the fulfillment of the appropriate boundary conditions.

The work is organized as follows. Section 2 describes the method, which includes the inversion procedure (2.1), the potential depuration (2.2) and its further optimization (2.3). Section 3 presents the resulting effective potentials for the orbitals corresponding to the ground states of different noble gases, including a thorough examination of the wavefunctions generated by these potentials (3.1). The corresponding exchange potentials are discussed in (3.2), comparing the potentials for specific– nl orbital with averaged potentials. Results of the same calculations for the Nitrogen atom are provided in (3.3). Atomic units are used unless otherwise specified.

2 THEORY

2.1 The direct inversion method

The radial part of the Schrödinger equation for an electron in a local and central potential is

$$\left[-\frac{1}{2} \frac{d^2}{dr^2} + \frac{l(l+1)}{2r^2} + V_{nl}(r) \right] u_{nl}(r) = \varepsilon_{nl} u_{nl}(r). \quad (1)$$

We assume the following hypothesis: If the wavefunctions u_{nl} are replaced by the solutions of an Hartree–Fock calculation u_{nl}^{HF} , then, the corresponding effective local potentials V_{nl}^{HF} that generate such wavefunctions should exist. Within this proposal we convert the HF method into a set of Kohn–Sham equations, whose solutions are the Hartree–Fock wavefunctions:

$$\left[-\frac{1}{2} \frac{d^2}{dr^2} + \frac{l(l+1)}{2r^2} + V_{nl}^{\text{HF}}(r) \right] u_{nl}^{\text{HF}}(r) = \varepsilon_{nl}^{\text{HF}} u_{nl}^{\text{HF}}(r). \quad (2)$$

The effective potentials given by,

$$V_{nl}^{\text{HF}}(r) = V^{\text{C}}(r) + V^{\text{dir}}(r) + V_{nl}^{\text{x}}(r), \quad (3)$$

are composed by the external potential V^{C} (the Coulomb field of the nucleus), the direct (or Hartree) potential V^{dir} (the electrostatic electron repulsion), and the orbital exchange potentials V_{nl}^{x} . We have ignored the correlation term since the HF solutions do not include it.

Since the solutions u_{nl}^{HF} are known (calculated numerically with the HF code by C. F. Fischer³⁴, and the NRHF code by W. Johnson³⁵) we could then proceed to invert directly

the Kohn–Sham equations:

$$V_{nl}^{\text{HF}}(r) = \frac{1}{2} \frac{1}{u_{nl}^{\text{HF}}(r)} \frac{d^2}{dr^2} u_{nl}^{\text{HF}}(r) - \frac{l(l+1)}{2r^2} + \varepsilon_{nl}^{\text{HF}}, \quad (4)$$

obtaining the *HF inverted potential* $V_{nl}^{\text{HF}}(r)$. Assuming a Coulombic–type shape, it is convenient to define an *HF inverted charge*

$$Z_{nl}^{\text{HF}}(r) \equiv -r V_{nl}^{\text{HF}}(r). \quad (5)$$

The direct computation of (4) is well known to pose serious numerical problems¹⁸. *First*, the presence of (genuine) nodes in the wave function to be inverted produces poles and unrealistic features around them. This has led to the general consensus that the inversion method can only be used for nodeless orbitals¹². *Second*, numerical rounding off of the exponential decay of the bound states hinders the corresponding inverted potential from having the physically desired asymptotic form. Moreover, there is a *third* problem and this is at the heart of the Hartree Fock method: the exact solutions may have oscillations (and therefore, spurious nodes) in the large- r or “tail” region of the functions. The existence of these spurious nodes in Hartree Fock was already suggested by Fischer³⁴. This failure is not rooted in the numerical scheme but it is inherent to the method. Probably, these nodes are surviving long-range exchange effects due to the non-local character of the Hartree–Fock wavefunctions: the behavior of a particular orbital depends on all others. We have found the same spurious nodes at the same places even by using the different numerical codes. As a general rule, the spurious nodes appear at very long distances, a region in which the amplitude of the wavefunction is very small. Therefore, their existence has no practical consequences, and they can be neglected in any general Hartree–Fock calculation. However, this is not true as far as the inversion procedure is concerned, as we will discuss in the next section.

2.2 The deputed inversion method

The mentioned difficulties make it very hard to obtain the correct V_{nl}^{HF} potentials by using the simple inversion given by Eq. (4). To overcome these troubles we have developed a deputed inversion method (DIM) which consists in optimizing the effective charges, rather than the effective potentials. Thus, we are able to constrain any potential to have the right boundary conditions, enforcing the *effective deputed inverted charge* behave as follows:

$$Z_{nl}^{\text{DIM}}(r) \rightarrow \begin{cases} Z_N & \text{as } r \rightarrow 0 \\ 1 & \text{as } r \rightarrow \infty \end{cases} \quad (6)$$

where Z_N is the nuclear charge. Once the charge is determined at the boundaries, we can obtain a smooth analytic expression for Z_{nl}^{DIM} , fitting the Z_{nl}^{HF} for the largest possible range, excepting in the neighborhood of the nodes. All this can be accomplished by imposing the effective DIM charge to fit the following analytical expression:

$$Z_{nl}^{\text{DIM}}(r) = \sum_j \alpha_j e^{-\beta_j r} + 1, \quad (7)$$

with $\sum_j \alpha_j = Z_N - 1$.

As an epitome of the numerical problems mentioned and the way proposed to solve them, we show, in Figure 1, the orbital u_{2s}^{HF} of the ground state of the Kr atom (part (a)), and its correspondent effective charge Z_{2s}^{HF} (dashed line curve, in part (b)). First, note that the $2s$ orbital has a genuine node at $r \approx 0.06$ a.u. which produces the first pole in the effective charge, as shown in the lower graph. The node appears at a relatively low- r value, so, the corresponding charge (see Eq. (5)) is not very sensitive to its presence. Therefore, it is very easy to eliminate the pole from the effective charge (by just erasing a few points around this radius).

All the bound wavefunctions decay exponentially beyond the last turning point. It is defined as the position r_{tp} in which the energy equals the effective potential. At first glance, it seems that the turning point of u_{2s} is located around $r_{tp} \approx 0.25$, and from that point on, the wavefunction should start to decay exponentially. From the numerical point of view, say $r \approx 10 r_{tp}$ is a good point to stop the inversion, since beyond there, the effective charge could begin to diverge.

Thus, naively, one might infer that by erasing the points belonging to the neighborhood of the first node, and by stopping the inversion about $10 r_{tp}$, the inversion procedure will work well. However, the dashed curve in Fig. 1(b) shows a completely unphysical Z_{2s}^{HF} resulting from the inversion. A very careful examination of the u_{2s}^{HF} orbital function evidences the presence of a spurious node at $r = 1.51$ a.u., in a region where the amplitude of the wavefunction is less than 10^{-4} times the maximum value (see the inset of Fig. 1(a)). Even though this node is completely innocuous for practical matters, it produces devastating effects in the inversion procedure, evidenced in the second huge peak in the Z_{2s}^{HF} curve (see Figure 1(b)). This pole is so big that affects a broad vicinity and causes the abrupt rising of the effective charge for $r > 0.5$ a.u.. This is really a surprising result since *a priori* there is no reason to suspect that a negligible oscillation in the tail of the wavefunction would produce such a big drawback at such a small distance as 0.5 a.u.. Care must be taken then to discard such an undesired effect.

2.3 Optimization

The adjustment of the parameters α_j and β_j requires some expertise. The key issue in the successful approximation is the region chosen for the fitting: it has to be as large as possible, in such a way that Z_{nl}^{DIM} overlaps with the inverted Z_{nl}^{HF} across a broad range, allowing an accurate fitting procedure, but discarding the points surrounding the nodes. Also, the inversion must be halted at a particular (as large as possible) r value, as soon as the amplitude of the function is too small. Going further, the inversion procedure diverges. Another issue to consider is the question of self consistency within the computer codes used in the calculations and the particular code used to generate the input wavefunctions. To that end, we opened up the Hartree–Fock codes^{34,35} and used the specific numerical grid including the derivatives at the same pivots. The optimization procedure is completed by a number of iteration steps, in which the parameters are optimized to give accurate energies and mean values.

It is important to state here that the majority of the density functional approximation

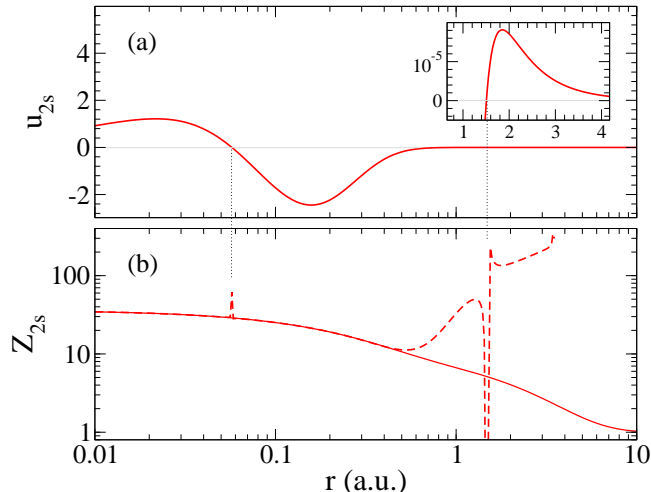


Figure 1: (a) Hartree-Fock orbital u_{2s}^{HF} corresponding to the ground state of the Kr atom. It presents two nodes, a genuine one at $r \approx 0.06$ a.u., and a spurious one at 1.51 a.u. (shown in the inset). (b) Dashed line: The corresponding inverted effective charge $Z_{2s}^{HF}(r)$, spoiled by the presence of poles. Solid line: Depurated $Z_{2s}^{DIM}(r)$ effective charge.

methods are based on a variational principle, minimizing the energy functionals. Without underestimating its importance, energy is only one of the many parameters that characterizes a quantum state. Different trial functions (having different forms) can produce, through a variational procedure, the same final energy. A simple example is given by Bartschat^{36,37} in which two different potentials (one having exchange, the other neglecting it) allowed to produce very similar and accurate energies of Rydberg series in several quasi-one electron systems. However, a further examination of these potentials shows large discrepancies in scattering calculations³⁸. Therefore, in addition to the energy values, we have included in our optimization method a variational procedure to reproduce accurately the mean values $\langle 1/r \rangle$ (which characterize the quality of the wavefunction near the origin), and $\langle r \rangle$, (probing it at longer distances).

The effective depurated inversion charge $Z_{2s}^{DIM}(r)$ corresponding to the 2s orbital of the Kr atom resulting from the optimization is shown –solid curve– in Figure 1(b). As seen in the figure, both boundary conditions are fulfilled (at the origin, $Z_{2s} \rightarrow 36$, and asymptotically $Z_{2s} \rightarrow 1$, as stated in Eq. (6)).

3 RESULTS

3.1 DIM Potentials, energies and mean values

The fitting parameters α_j and β_j defining the effective charges $Z_{nl}^{DIM}(r)$ in Eq. (7) for the noble gases Helium, Neon, Argon and Krypton, are given in Table 1. We have limited the α_j and β_j to six (about a couple per shell). For Kr, we would probably need an additional couple since there are four shells involved. Having these effective charges, we built the corresponding DIM potentials V_{nl}^{DIM} . By solving the Schrödinger equation (Eq. (1)), we obtained the

Table 1: Fitting parameters for the effective charge $Z_{nl}^{\text{DIM}}(r)$ for He, Ne, Ar, and Kr, by using Eq. (7).

	nl	α	β		nl	α	β
He	1s	-0.31745	5.04372	Kr	1s	5.49263	0.884768
		1.31745	2.50032			3.94437	16.8769
		-	-			25.5630	3.10032
Ne	1s	7.367687	2.417275	2s	9.63120	0.575832	
		1.300360	0.126396		1.84650	25.53280	
		0.331953	13.15820		23.5223	4.543350	
	2s	0.297739	17.99390	2p	3.20530	20.83535	
		0.668081	0.067288		23.6172	3.928520	
		8.03418	2.47221		8.17750	0.636486	
	2p	1.353049	8.56948	3s	6.52203	0.547357	
		0.335881	0.464942		24.4475	3.657030	
		7.311070	2.090634		4.03047	16.61770	
Ar	1s	6.727570	6.177720	3p	23.13135	4.010523	
		4.751090	1.343560		3.325360	20.41890	
		5.521340	0.859981		8.543290	0.821218	
	2s	8.90271	1.09779	3d	10.05320	1.04843	
		2.36850	2.93144		21.81544	4.25746	
		5.72879	6.95913		3.131360	20.6087	
	2p	4.96956	6.14455	4s	3.65988	0.49000	
		1.48464	10.86843		26.4565	3.17799	
		10.5458	1.30005		4.88362	15.2031	
	3s	10.3202	2.33169	4p	7.35713	1.00142	
		4.27115	7.33678		24.2321	3.7309	
		2.40865	0.407463		3.41077	22.5680	
	3p	8.43753	3.49259				
		2.18200	10.8595				
		6.38047	1.07080				

solutions $u_{nl}^{\text{DIM}}(r)$ and the corresponding energies $\varepsilon_{nl}^{\text{DIM}}$ and the mean values $\langle r \rangle$ and $\langle 1/r \rangle$. The fitting procedure allows us to reproduce the original Hartree–Fock wavefunctions with a remarkable degree of accuracy. The comparisons between the results obtained from the diagonalization of the Hamiltonian with the $V_{nl}^{\text{DIM}}(r)$ effective potential and the original Hartree–Fock orbitals are presented in Table 2. It is remarkable that with such simple analytical expressions for the potentials we are able to reproduce exactly the same energies as the HF method. The only exception is the $4p$ orbital of Kr, in which both calculations agree up to the fifth significant figure. The fitting procedure also allows to reproduce the original HF wavefunctions with an outstanding degree of accuracy. The mean values $\langle r \rangle$ obtained with the DIM effective potentials agree with the HF values in about 0.1%. A similar scenario is achieved for the $\langle 1/r \rangle$ mean values.

Finally, we calculated the total energy for the ground state of each atom, by using the following expression:

$$E^{\text{DIM}} = \sum_{nl} \left[\varepsilon_{nl}^{\text{DIM}} - \frac{1}{2} \int \rho_{nl}^{\text{DIM}}(r) \left(V_{nl}^{\text{DIM}}(r) + \frac{Z_N}{r} \right) dr \right], \quad (8)$$

where the density $\rho_{nl}^{\text{DIM}}(r) = |u_{nl}^{\text{DIM}}(r)|^2$. The calculated energies E^{DIM} are given in Table 3, together with the total energies obtained by the Hartree–Fock calculations (labeled as E^{HF}). The comparisons show a notable agreement between both calculations. However, it is worth investigating whether (the very small) discrepancies originate from the determination of the DIM potentials, or from their diagonalized wavefunctions u_{nl}^{DIM} . For this purpose, we replaced in Eq. (8) the ρ^{DIM} by the density ρ^{HF} calculated from the original u_{nl}^{HF} functions. We labelled these resulting total energies as $E_{\rho^{\text{HF}}}^{\text{DIM}}$. As seen in the table, for He and Ne these energies are exactly the same as the HF energies. For Ne and Kr, the discrepancies between them are of the order of $10^{-4}\%$. These results prove without any doubt the high quality of the potentials generated by our method.

3.2 The exchange potential

Due to the fact that the Hartree–Fock method does not take into account the correlations, our procedure allows us to extract the exchange potential $V_{nl}^{\text{DIMx}}(r)$ “exactly”, for each nl orbital

$$V_{nl}^{\text{DIMx}}(r) = V_{nl}^{\text{DIM}}(r) + \frac{Z_N}{r} - \int \frac{\rho^{\text{HF}}(r')}{|\mathbf{r} - \mathbf{r}'|} d\mathbf{r}', \quad (9)$$

where $\rho^{\text{HF}}(r)$ is the total density calculated with the u_{nl}^{HF} wavefunctions.

Obviously, orbital–specific exchange potentials can be obtained exactly by computing the Fock exchange operator. However, these potentials are rather difficult to put in a simple and smooth analytical expression such as Eq. (7), due to the presence of nodes and other features discussed in this work. An exact average exchange potential can be calculated through the average exchange charge density proposed by Slater³⁹,

$$V_S^{\text{x}}(r) = \frac{1}{\rho(r)} \sum_i \sum_j \int \frac{u_i^*(r) u_j^*(r') u_j(r) u_i(r')}{|\mathbf{r} - \mathbf{r}'|} d\mathbf{r}'. \quad (10)$$

Table 2: Energy and mean values for He, Ne, Ar and Kr atoms obtained from DIM effective potentials (upper rows) compared with the original Hartree–Fock values (lower rows).

nl		ϵ^{DIM}	$\langle r \rangle^{\text{DIM}}$	$\langle 1/r \rangle^{\text{DIM}}$	
		ϵ^{HF}	$\langle r \rangle^{\text{HF}}$	$\langle 1/r \rangle^{\text{HF}}$	
He	1s	-0.917956	0.927313	1.687251	
		-0.917956	0.927273	1.687282	
Ne	1s	-32.772447	0.157491	9.621450	
		-32.772443	0.157631	9.618054	
	2s	-1.930391	0.891336	1.640769	
		-1.930391	0.892113	1.632553	
	2p	-0.850410	0.967755	1.430252	
		-0.850410	0.965274	1.435350	
Ar	1s	-118.610352	0.086015	17.561606	
		-118.610350	0.086104	17.553229	
	2s	-12.322153	0.411857	3.562264	
		-12.322153	0.412280	3.555317	
	2p	-9.571466	0.375269	3.449283	
		-9.571466	0.375330	3.449989	
	3s	-1.277353	1.426944	0.967005	
		-1.277353	1.422172	0.961985	
	3p	-0.591017	1.668648	0.817928	
		-0.591017	1.662959	0.814074	
	Kr	1s	-520.165467	0.042441	35.483699
			-520.165468	0.042441	35.498152
2s		-69.903081	0.187181	7.924967	
		-69.903082	0.187256	7.918830	
2p		-63.009784	0.161695	7.874355	
		-63.009785	0.161876	7.868429	
3s		-10.849466	0.537875	2.644610	
		-10.849466	0.537802	2.637556	
3p		-8.331501	0.542133	2.530080	
		-8.331501	0.542627	2.522775	
3d		-3.825234	0.550922	2.276713	
		-3.825234	0.550880	2.276940	
4s		-1.152935	1.630081	0.808453	
		-1.152935	1.629391	0.804188	
4p		-0.524186	1.950193	0.675555	
		-0.524187	1.951611	0.669219	

Table 3: Total energies (in a.u.) for the ground states of He, Ne, Ar and Kr atoms, given by Eq. (8). For comparisons, $E_{\rho^{\text{DIM}}}^{\text{DIM}}$ (where ρ^{HF} replaces the ρ^{DIM} densities), and the Hartree–Fock total energies E^{HF} are also given.

Atom	E^{DIM}	$E_{\rho^{\text{HF}}}^{\text{DIM}}$	E^{HF}
He	-2.8616	-2.8617	-2.8617
Ne	-128.4978	-128.5475	-128.5475
Ar	-526.8030	-526.8198	-526.8175

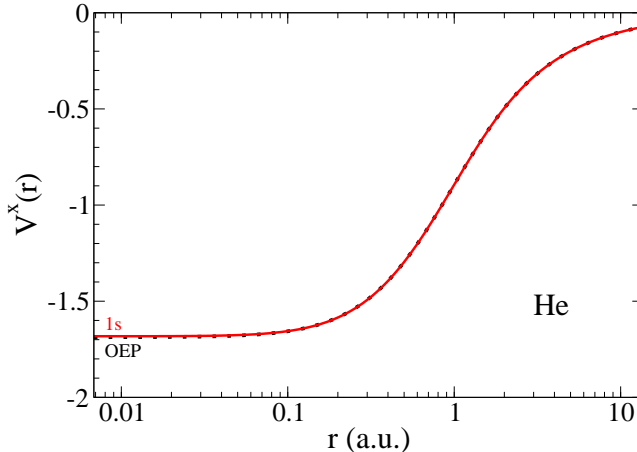


Figure 2: (color online). Orbital-specific exchange potential $V_{1s}^{\text{DIMx}}(r)$, and V_{OEP}^x , for the ground state of He.

Our approach, on the other hand, allows us to obtain orbital-specific singularity-free exchange potentials straightforwardly.

According to Eq. (9) all orbital-specific potentials should approach the same value at $r = 0$, because $Z_{nl}^{\text{DIM}}(r) = rV_{nl}^{\text{DIM}}(r)$ approaches Z_N regardless of nl (the other terms are the same for every orbital). However, from Figs 3 to 5 it appears that the potentials for the different orbitals approach different values at the origin. This is a consequence of the fact that every DIM potential tends to Z_N with different behavior, determined by their fitting parameters. In fact, for very low r values $V_{nl}^{\text{DIM}}(r) \approx \sum_j \alpha_j \beta_j - V^d(r)$, but they have strictly the same value at $r = 0$.

Figures 2 to 5 show the orbital-specific exchange potentials $V_{nl}^{\text{DIMx}}(r)$ for the ground states of the four noble gases He, Ne, Ar, and Kr, calculated with the depurated inversion method DIM. In order to compare our results, we also calculated the widely used optimized effective potential (OEP) developed by Talman⁶, displayed in the figures with dotted lines. It is well known that the OEP potential works reasonably well for the outer shell but poorly for the inner ones. Since this potential is calculated by averaging the different nl -orbitals, it is closer, at very low radius, to the s -orbitals (the only orbitals having a non-negligible probability). At longer distances, all the nl orbitals have a similar behavior accompanying the OEP exchange potential.

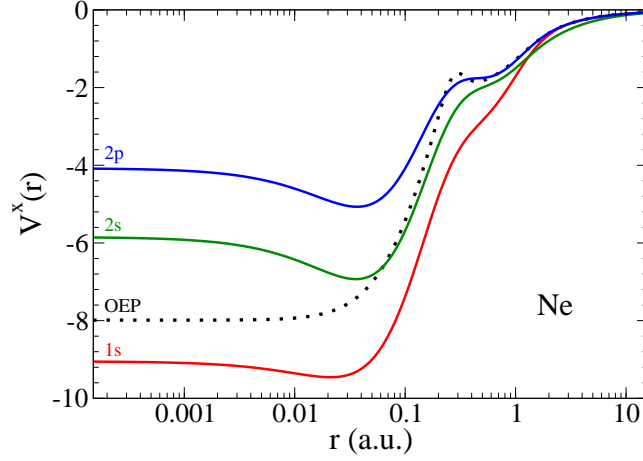


Figure 3: (color online). Orbital-specific exchange potentials $V_{nl}^{\text{DIM}x}(r)$, and V_{OEP}^x , for the ground state of Ne.

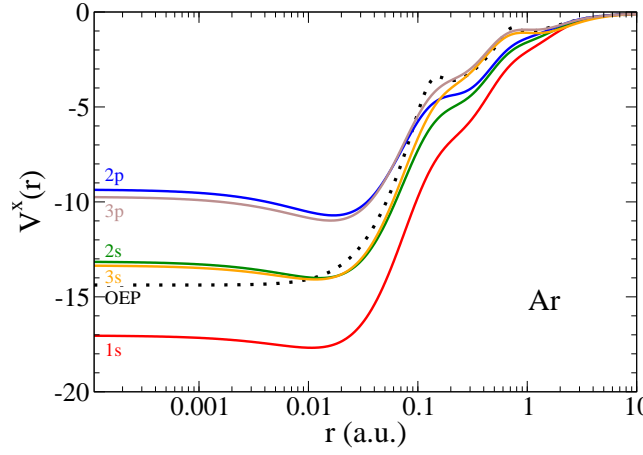


Figure 4: (color online). Orbital-specific exchange potentials $V_{nl}^{\text{DIM}x}(r)$, and V_{OEP}^x , for the ground state of Ar.

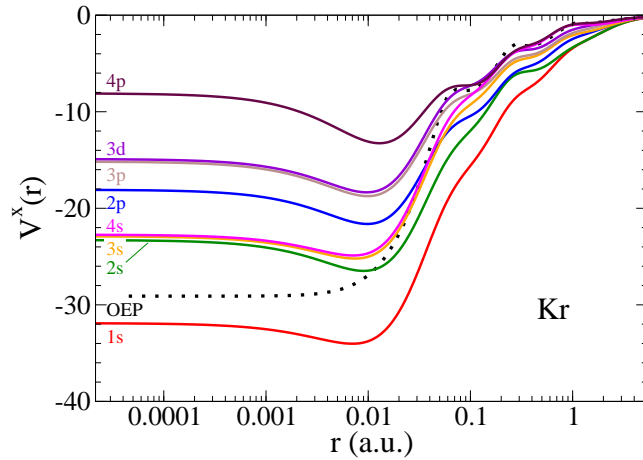


Figure 5: (color online). Orbital-specific exchange potentials $V_{nl}^{\text{DIM}x}(r)$, and V_{OEP}^x , for the ground state of Kr.

Table 4: Orbital and total exchange energies for He, Ne, Ar, and Kr.

	l	n				Total	EAHF
		1	2	3	4		
He	0	-0.5129				-1.0258	-1.026
Ne	0	-3.1106	-0.8620			-12.1080	-12.11
	1		-0.6938				
Ar	0	-5.8760	-1.9470	-0.5742		-30.1826	-30.19
	1		-1.7974	-0.4340			
Kr	0	-12.2258	-4.5523	-1.9972	-0.5275	-93.8525	-93.89
	1		-4.4305	-1.8401	-0.3906		
	2			-1.5280			

As a final test for our method, we calculated the total exchange energy E^x as given by,

$$E^x = \sum_{nl} E_{nl}^x = \sum_{nl} \left[\frac{1}{2} \int \rho_{nl}^{\text{HF}}(r) V_{nl}^{\text{DIMx}}(r) dr \right] \quad (11)$$

Table 4 displays the orbital exchange energy as well as the total exchange energy for He, Ne, Ar and Kr. The total exchange energies are compared with the exact atomic Hartree–Fock (EAHF) values given by Becke⁴⁰. The agreement is very good, of about 10⁻²%.

3.3 Nitrogen DIM and Exchange Potentials

The lower configuration $2p^3$ of Nitrogen gives rise to three different terms: 2^4S , 2^2D , 2^2P . Each of them is described by a different electronic density. The fitting parameters that define the term–dependent effective charges are given in Table 5 for each of the terms. We built the corresponding DIM potentials from these effective charges. By using these potentials we solved the Schrödinger equation (Eq.(1)) for every term, obtained the solutions, the energies, and the corresponding mean values $\langle r \rangle$ and $\langle 1/r \rangle$. The comparisons between the orbitals obtained from the diagonalization of the Hamiltonian with the effective potentials and the original Hartree–Fock orbitals are shown in Table 6. The mean values $\langle r \rangle$ obtained with the DIM effective potentials agree with the HF values in about 0.1%, and the $\langle 1/r \rangle$ mean values agree in about 0.2%.

The calculated total energies E^{DIM} for each term of the Nitrogen atom using Eq. (11) are presented in Table 7. Once again, in order to compare the quality of our method we calculated $E_{\rho_{\text{HF}}}^{\text{DIM}}$. The agreement between the DIM total energies and the original HF total energies is excellent, of about 10⁻⁴%.

Since Hartree–Fock does not consider correlations, the “exact” nl –orbital exchange potential for every term can be obtained. Figure 6 shows the nl –orbital exchange potentials for the 2^4S , 2^2D and 2^2P terms, calculated with the deperated inversion method. Again, to compare our results, the exchange potential given by Talman⁶ (OEP) is presented in the figures in light grey. Figure 6(a) illustrates the exchange potential for the $1s$ orbitals for the different terms, showing an overall similarity. The OEP potential behaves like the $V_{1s}^{\text{xDIM}}(r)$

Table 5: Fitting parameters for the effective charge $Z_{nl}^{\text{DIM}}(r)$ for 2^4S , 2^2D and 2^2P terms of Nitrogen.

	2^4S		2^2D		2^2P	
nl	α	β	α	β	α	β
$1s$	5.25634	1.26207	5.18635	1.22410	5.18635	1.21779
	0.743660	8.02844	0.813650	7.56800	0.813650	7.56740
$2s$	2.45281	3.51271	0.398100	0.239738	0.890660	0.830615
	0.833570	3.38654	1.85412	1.03105	3.66999	3.14946
	2.71362	0.894699	3.74778	2.85313	1.43935	0.740427
$2p$	3.64345	1.24069	4.01052	1.28744	1.89769	1.16557
	2.05501	5.35135	1.85517	5.70858	1.77430	5.68782
	0.301540	0.286609	0.134310	0.267987	2.32801	1.40925

Table 6: Energy and mean values for the 2^4S , 2^2D and 2^2P terms of N obtained from the DIM effective potentials (upper rows) compared with the Hartree–Fock values (lower rows).

nl	ϵ^{DIM}	$\langle r \rangle^{\text{DIM}}$	$\langle 1/r \rangle^{\text{DIM}}$	$\langle r^2 \rangle^{\text{DIM}}$	
	ϵ^{HF}	$\langle r \rangle^{\text{HF}}$	$\langle 1/r \rangle^{\text{HF}}$	$\langle r^2 \rangle^{\text{HF}}$	
2^4S	$1s$	-15.629060	0.228296	6.648629	0.070199
		-15.629060	0.22830	6.65324	0.07027
	$2s$	-0.945324	1.334474	1.080369	2.145339
		-0.945324	1.33228	1.07818	2.14944
	$2p$	-0.567589	1.412683	0.954982	2.555457
		-0.567589	1.40963	0.95769	2.54766
2^2D	$1s$	-15.666392	0.228290	6.649289	0.070200
		-15.666392	0.22826	6.65388	0.07024
	$2s$	-0.963670	1.329174	1.086439	2.134548
		-0.963670	1.32632	1.08318	2.12941
	$2p$	-0.508655	1.448778	0.938821	2.709128
		-0.508655	1.44662	0.94208	2.70716
2^2P	$1s$	-15.691599	0.228242	6.650362	0.070167
		-15.691599	0.22824	6.65430	0.07022
	$2s$	-0.976339	1.325618	1.087123	2.115849
		-0.976339	1.32232	1.08656	2.11600
	$2p$	-0.471297	1.471755	0.929822	2.811999
		-0.471297	1.47301	0.93155	2.82518

Table 7: Total energies (a.u.) for the 2^4S , 2^2D and 2^2P terms of Nitrogen.

	E^{DIM}	$E_{\rho^{\text{HF}}}^{\text{DIM}}$	E^{HF}
2^4S	-54.376170	-54.400833	-54.400934
2^2D	-54.275569	-54.296587	-54.296169
2^2P	-54.208564	-54.228313	-54.228102

Table 8: Orbital and total exchange energies for 2^4S , 2^2D and 2^2P terms of Nitrogen.

	1s	2s	2p	Total	EAHF
2^4S	-2.1175	-0.4776	-0.4711	-6.6034	-6.596
2^2D	-2.1175	-0.4777	-0.4262	-6.4688	
2^2P	-2.1175	-0.4780	-0.3073	-6.3027	

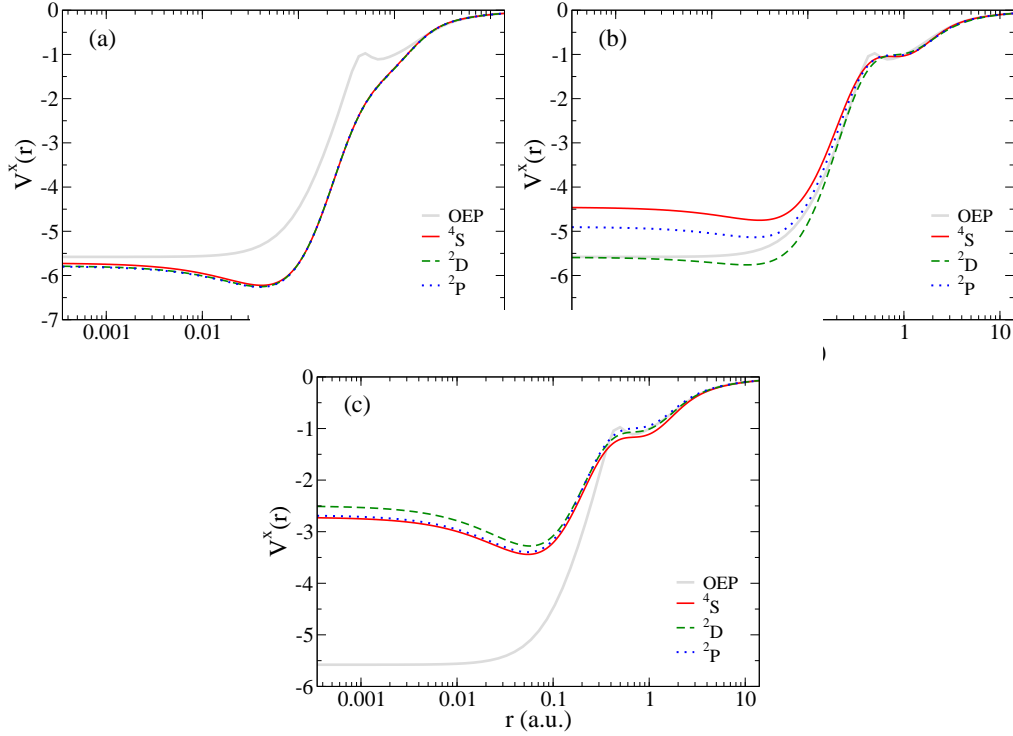


Figure 6: (color online). DIM exchange potential $V_{nl}^{\text{DIM}x}(r)$ for the (a) $1s$, (b) $2s$ and (c) $2p$ orbitals, for the 2^4S , 2^2D and 2^2P terms of Nitrogen.

only at short and large distances. Figure 6(b) shows the exchange potentials for the $2s$ orbitals. In this case, noticeable differences between the term-potentials rise at low values of r . For r higher than 0.5 a.u., all the term-potentials become indistinguishable and agrees perfectly with the OEP potential. A peculiarity observed in the figure is that the OEP potential agrees very well with the $V_{2s}^{\text{DIM}x}(r)$ for the 2^2D term. Figure 6(c) displays the $2p$ exchange potentials, which behave similarly for all the terms. However, since the OEP potential is the same for all the orbitals and terms, it disagrees completely with the $V_{2p}^x(r)$ at short distances.

Table 8 presents the total exchange energy and the nl -exchange energies of the 2^4S , 2^2D and 2^2P terms. The $1s$ -exchange energy for all the terms are the same, as expected for a closed-shell orbital. Similarly, the $2s$ -exchange energy vary slightly, with a difference of 0.08%. However, this is not the case for the $2p$ -exchange energy, which vary significantly, having discrepancies of about 18% between the different terms. The total exchange energy computed with Eq. (11) for the terms are compared with the exact atomic Hartree-Fock (EAHF) exchange energy, with an agreement of about 0.1%.

4 CONCLUSIONS

To attain an accurate representation of the exchange functional is at the heart of the density functional method. On the other hand, the atomic collision community needs accurate one-electron potentials allowing to generate the bound and continuum states on the same footing for further calculations of collisional processes. These potentials need to be resolved for any nl -specific orbital, a quality lacking in the chemistry community functionals. In the present work we devised and implemented a depurated inversion method, which allows to obtain the sought potentials through a very simple analytical expression of the effective charges. The method consists in the inversion of a Kohn–Sham equation, in which the KS orbitals have been replaced by the Hartree–Fock orbitals. By means of diagonalization we have achieved accurate wavefunctions having almost perfect agreement with the original Hartree–Fock wave functions. The quality of the potentials obtained by the present method is remarkably good. We applied the developed methodology to the calculation of the ground state orbitals of noble gases and the Nitrogen atom. It is worth mentioning that the same technique can be used for any other atom, and for any other level, i.e., it is not limited to the ground state, as is the case in many of the existing exchange functionals.

ACKNOWLEDGMENTS

This work was supported by grants of CONICET, ANPCyT, and UBACyT, of Argentina.

References

- [1] Becke, A.D. *J. Chem. Phys.* 2014, 140, 18A301.
- [2] Bartlett, R.J. *Mol. Phys.* 2010, 108, 3299-3311.
- [3] Verma, P.; Bartlett, R.J. *J. Chem. Phys.* 2012, 137, 134102.
- [4] Sharp, R.T.; Horton, G.K. *Phys. Rev.* 1953, 90, 317.
- [5] Talman, J.D.; Shadwick, W.F. *Phys. Rev. A* 1976, 14, 36-40.
- [6] Talman, J.D. *Comput. Phys. Commun.* 1989, 54, 85-94.
- [7] Görling, A. *Phys. Rev. A* 1992, 46, 3753-3757.
- [8] Krieger, J.B.; Li, Y.; Iafrate, G.J. *Phys. Rev. A* 1992, 45, 101-126.
- [9] Yang, W.; Wu, Q. *Phys. Rev. Lett.* 2002, 89, 143002.
- [10] V.N. Staroverov and G.E. Scuseria, *J. Chem. Phys.* 2006, 125, 081104.
- [11] I.G. Ryabinkin, A.A. Kananenka, and V.N. Staroverov, *Phys. Rev. Lett.* 2013, 111, 013001.

- [12] A.A. Kananenka, S.V. Kohut, A.P. Gaiduk, and I.G. Ryabinkin, *J. Chem. Phys.* 2013, 139, 074112.
- [13] ABINIT, www.abinit.org
- [14] Vanderbilt Ultra-Soft Pseudopotential, www.physics.rutgers.edu/~dhv/uspp/
- [15] Gaiduk, A.P.; Ryabinkin, I.G.; Staroverov, V.N. *J. Chem. Theory Comput.* 2013, 9, 3959.
- [16] Wu, Q.; Yang, W. *J. Chem. Phys.* 2003, 118, 2498.
- [17] Ryabinkin, I.G.; Kohut, S.V. Staroverov, V.N. *Phys. Rev. Lett.* 2015, 115, 083001.
- [18] Mura, M.E.; Knowles, P.J.; Reynolds, C.A. *J. Chem. Phys.* 1997, 106, 9659.
- [19] Umrigar, C.J.; Gonze, X. *Phys. Rev. A* 1994, 50, 3827.
- [20] Gritsenko, O.V.; Baerends, E.J. *Theor. Chem. Acc.* 1997, 96, 44.
- [21] Filippi, C.; Umrigar, C.J.; Taut, M. *J. Chem. Phys.* 1994, 100, 1290.
- [22] P. de Silva and T.A. Wesolowski, *Phys. Rev. A* 2012, 85, 032518.
- [23] Schipper, P.R.T.; Gritsenko, O.V.; Baerends, E.J. *Theor. Chem. Acc.* 1997, 98, 16.
- [24] Jacob, C.R. *J. Chem. Phys.* 2011, 135, 244102.
- [25] Hilton, P.R.; Nordholm, S.; Hush, N.S. *J. Chem. Phys.* 1997, 67, 5213.
- [26] Süzer, S.; Hilton, P.R.; Hush, N.S.; Nordholm, S. *J. Elect. Spec. Rel. Phen.* 1977, 12, 357.
- [27] Hilton, P.R.; Nordholm, S.; Hush, N.S. *Chem. Phys. Lett.* 1979, 64, 515.
- [28] Hilton, P.R.; Nordholm, S.; Hush, N.S. *J. Elect. Spec. Rel. Phen.* 1980, 18, 101.
- [29] Crljen, Ž.; Wendin, G. *Phys. Rev. A* 1987, 35, 1571.
- [30] Sternheimer, R.M. *Phys. Rev.* 1954, 96, 951.
- [31] Dalgarno, A.; Parkinson, D. *Proc. R. Soc. Lond. A* 1959, 250, 422.
- [32] Barone, V. *J. Chem. Phys.* 1994, 101, 6834.
- [33] Kaupp, M.; Arbuznikov, A.V.; Heßelmann, A.; Görling, A. *J. Chem. Phys.* 2010, 132, 184107.
- [34] Froese Fischer, C.; Brage, T.; Jönsson, P. *Computational Atomic Structure, an MCHF approach*, Institute of Physics Publishing, 1997.
- [35] Johnson, W.R. *Atomic Structure Theory: Lectures on Atomic Physics*, Springer, 2007.

- [36] Albright, B.J.; Bartschat, K.; Flicek, P.R. *J. Phys. B* 1993, 26, 337.
- [37] Bartschat, K. *Computational Atomic Physics*, Springer–Verlag, 1996; Chapter II.
- [38] Bartschat, K.; Bray, I. *J. Phys. B* 1996, 29, 271.
- [39] Slater, J.C. *Phys. Rev.* 1981, 81, 385.
- [40] Becke, A.D. *Phys. Rev. A* 1988, 38, 3098.